

2D-segmented, multi-TE 3D-EPI for high-resolution R_2^* and quantitative susceptibility mapping at 7 Tesla

Rüdiger Stirnberg¹, Julio Acosta-Cabronero², Benedikt A. Poser³, and Tony Stöcker^{1,4}

¹German Center for Neurodegenerative Diseases (DZNE), Bonn, Germany, ²German Center for Neurodegenerative Diseases (DZNE), Magdeburg, Germany, ³Faculty of Psychology and Neuroscience, Maastricht University, Maastricht, Netherlands, ⁴Department of Physics and Astronomy, University of Bonn, Bonn, Germany

Target Audience: Neuroscientists and MR physicists interested in fast and robust R_2^* and quantitative susceptibility mapping at high and ultra-high fields.

Purpose: To investigate the feasibility of using slice- and in-plane segmented three-dimensional echo planar imaging (3D-EPI)¹ for high-resolution quantitative susceptibility mapping (QSM) and R_2^* relaxation rate mapping at 7 Tesla. It has previously been shown that conventional 3D-EPI (segmentation along secondary phase encoding direction, PE2, only)³ is suitable for QSM at 3 Tesla², resulting in acquisition times (TA) that are only a fraction of those with conventional gradient echo (GRE). Moving to higher field strengths requires shorter echo times (TEs) and usually involves higher spatial resolutions. The present work explored the use of additional in-plane segmentation along the primary phase encoding direction (PE1) and higher parallel imaging (PI) acceleration to meet both requirements for QSM/ R_2^* measurements at 7T.

Methods: A 3D-EPI sequence was extended by in-plane segmentation¹: instead of acquiring complete k-space data according to one PE2 step in one EPI run, it is acquired in N_s successive runs with an N_s -fold larger gap between PE1 steps and an adjusted PE1 offset. This includes appropriate echo time shifting (ETS)⁴. Together with R-fold in-plane PI acceleration this corresponds to only every $(N_s \cdot R)$ th PE1 line acquired within one run (increased PE1 bandwidth). The sequence allows for easy expansion to multiple R_2^* weightings by looping over different TEs over measurements (adapted pre- and post-EPI-readout fill times, cf. Fig. 1). A constant TR_{shot} guarantees an unperturbed steady-state throughout the entire experiment.

EXPERIMENT 1 (QSM): All experiments were performed on one experienced subject using a 7T human research scanner (Siemens) equipped with a 70mT/m gradient system and a 32 channel head receive coil (Nova Medical). A series of single-TE 2D-segmented 3D-EPI scans optimized for susceptibility weighting were acquired for later comparison to a reference GRE with matched parameters: strict axial slice orientation (PE1:A>P, PE2:I>S), 240x240x80 matrix, 10% slice oversampling, 0.8x0.8x1.6mm³ voxel, TE=11ms, R=3 (GRAPPA reconstruction⁵). Differing parameters (GRE/EPI): readout bandwidth (130/1230)Hz/pixel, $TR_{\text{shot}}=(20/21.4)$ ms, nominal flip angle (FA 10°/11°), measurements (1/10), TA (3:17/3:11)min. **EPI-specific:** $N_s=9$, $TR_{\text{vol}}=16.9$ s. Whereas for GRE 48x24 integrated GRAPPA reference lines were scanned (with SNR benefit), for 3D-EPI they were pre-scanned in an $R \times N_s$ -fold in-plane segmented fashion following 150 dummy shots (21.5s pre-scan time). Magnitude and phase data from each receive channel were stored and combined off-line for optimal phase reconstruction⁶. Subsequently, linear phase trend removal and cumulative complex averaging (across 1-10 measurements) were carried out. Finally, a *state-of-the-art* processing pipeline was used to invert local susceptibility sources from the cumulative EPI and GRE datasets; in short: Laplacian phase unwrapping⁷, background field removal (PDF method)⁸; QSM inversion by noise-matched regularization (MEDIN approach)⁹. Mean susceptibility and standard deviation are computed from four matched regions of interest in GRE and 3D-EPI.

EXPERIMENT 2 (R_2^*): A two-TE, 1mm isometric whole-brain protocol with 17 measurements was performed. TE($n=1,3,\dots,17$)=23ms, TE($n=2,4,\dots,16$)=39ms, 192x192x128 matrix, 12.5% slice oversampling, R=3, $N_s=2$, $TR_{\text{vol}}=15.34$ s, readout bandwidth 1090Hz/pixel, nominal FA 16°, TA=4:43min. R_2^* was calculated from a linear fit on the logarithm of the first 2-17 magnitude images.

Results: All QSM reconstructions are qualitatively concordant (cf. Fig. 2) with minimal geometric distortions in 3D-EPI (in A>P direction) and GRE (in L>R direction), respectively. Regional plots demonstrate 3D-EPI stability and relative consistency with GRE-based QSM. A single EPI scan (TA=0:38min) is remarkably accurate when compared to ten averages (TA=3:11min). In contrast, R_2^* estimates from the two-TE protocol improve notably through repetitions (cf. Fig. 3).

Discussion: We have demonstrated at 7T that, depending on the application, the SNR deficit due to higher readout bandwidths with 2D-segmented 3D-EPI compared to conventional GRE can be compensated for by averaging or fitting of only two to four scans with a single or multiple R_2^* weightings. Specifically for QSM we found that a single 3D-EPI measurement returns reliable values in sub-minute acquisition times, suggesting the proposed approach could be extended as a fast implementation for susceptibility tensor imaging¹⁰. Alternatively, the reduced motion sensitivity of 3D-EPI, which is particularly important for high-resolution imaging, enables the user to work on scan redundancy with non-cooperative subjects. Non-motion-corrupted volumes can be coregistered before QSM mapping (real and imaginary part) or individual QSM maps could be averaged. The latter approach would allow for updating the main field direction (correct dipole inversion). Furthermore, higher slice resolutions in relatively short scan time are feasible, thus enabling post-hoc sliding-window averaging in slice direction, if necessary. It should be noted that the above applications would be equally relevant at lower field strengths.

Conclusion: The relatively low acquisition efficiency and high motion sensitivity of GRE can be overcome by multiple 2D-segmented 3D-EPI acquisitions of exactly as many k-space lines as can possibly be acquired within optimal TE (and TR). The proposed approach yielded high quality QSM and R_2^* maps at 7T.

References: [1] Stirnberg et al., ISMRM, 2013; [2] Bredies et al., ISMRM, 2014; [3] Poser et al., NeuroImage, 2010; [4] Hennel, CMR, 1997; [5] Griswold et al., MRM, 2002; [6] Yang et al., ISMRM, 1999; [7] Schofield & Zhu, Opt Lett 2003; [8] Liu et al. NMR Biomed 2011; [9] Liu et al., MRM 2013; [10] Liu, MRM, 2010

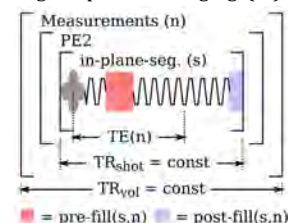


Fig. 1 Loop structure of multi-TE 2D-segmented 3D-EPI. Primary PE is performed during EPI readout.

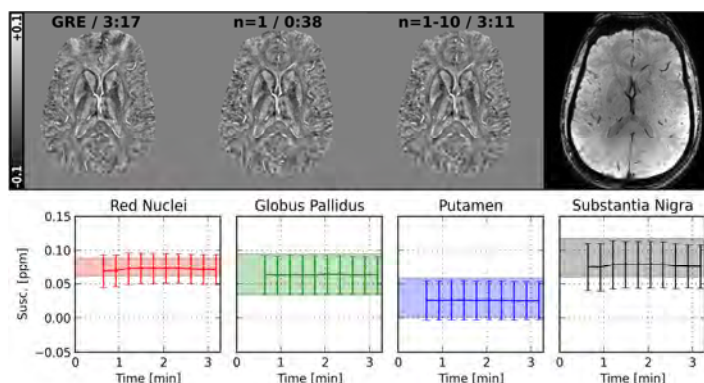


Fig. 2 Top: QSM maps in [ppm] of GRE (left) and EPI for $n=1$ and 10 averages (acquisition time in [min]:[s]). Right: 10 average EPI magnitude. Bottom: susceptibility mean \pm std obtained from different ROIs plotted vs. acquisition time (increasing number of averages). The width and height of the shaded area reflects the GRE acquisition time as well as the respective mean \pm std interval.

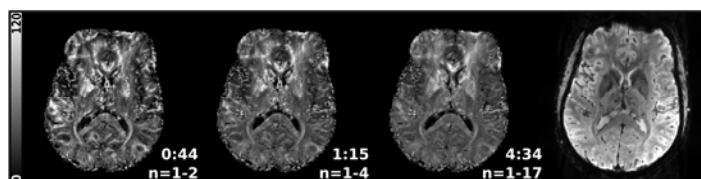


Fig. 3 R_2^* maps [s^{-1}] obtained from $n=2, 4$ or 17 measurements using two-fold in-plane segmented 3D-EPI with TE=23ms and 39ms. Respective TAs are given in [min]:[s]. The map converges after 4-8 measurements. Right: simple magnitude sum yields superior image contrast with mixed R_2^* weighting.